scientific reports

Check for updates

OPEN

Integrating physiological and anatomical insights to unveil the mechanism of coloration in *Prunus sibirica*

Wenxuan Fan[1,2], Yuncheng Zhang[3], Jianhua Chen[1,2]✉, Junxin Feng[1,2], Jindi Yang[1,2], Yongqiang Sun[1,2] & Shengjun Dong[1,2]✉

Pink-flowered *Prunus sibirica*, of the genus *Prunus*, is an exceptional germplasm resource with high ornamental value. Understanding the mechanism behind petal coloration is crucial for cultivating ornamental *P. sibirica* varieties. This study utilized pink-flowered and white-flowered *P. sibirica* petals at different stages of flowering to explore the relationship between various physiological indicators, anatomical structures of petals, and flower coloration during flowering. Results indicated that anthocyanins, key pigment indicators in pink-flowered *P. sibirica*, directly influenced the *a values (redness). Increased activity of phenylalanine deaminase (4.43–29.69 U/g), chalcone isomerase (9.80–46.67 U/g), and soluble sugar content (29.25–35.28 mg/g) promoted anthocyanin synthesis and accumulation. These substances indirectly affected flower color by influencing anthocyanin content through physiological processes related to petal coloration. Structural changes in epidermal cells of pink and white flower petals during flowering were similar, with differences in pigment content and distribution impacting petal light absorption. Correlation analysis revealed that *a** values were significantly and positively correlated with five factors, one of which was anthocyanin content, and significant negative correlations with soluble protein content and cytosol pH. This study examined the factors influencing petal coloration in pink-flowered *P. sibirica* from both physiological and anatomical perspectives, providing a theoretical foundation for breeding new varieties of ornamental flowering plants.**

Keywords *Prunus sibirica*, Petal coloration, Anthocyanin, Anatomical structure

Prunus sibirica, a wild plant belonging to the genus *Prunus* of the Rosaceae family, is primarily found in three northern regions of China. Known for its cold and drought resistance, adaptability, and soil conservation properties[1], it is a key species for afforestation and ecological restoration projects. Besides its ecological significance, *P. sibirica*, particularly the pink-flowered variety, is valued for its ornamental qualities. The pink-flowered *P. sibirica* exhibits distinct physiological characteristics, making it more preferable to the common variety. When in full bloom, its petals (5–10), veins, and stamens are a bright pink, enhancing its ornamental appeal[2]. Current research on *P. sibirica* blossoms focus on its cold tolerance[3], regulation of its flowering genes[4], and pistil abortion[5]. However, the underlying mechanisms governing the coloration of the pink-flowered *P. sibirica* remain unexplored.

Flower coloration, regulated by various factors, is a crucial characteristic of ornamental plants[6]. Recent research highlights the significant role of pigments in determining flower color[7]. These pigments, classified as flavonoids, carotenoids, and betaines[8], influence flower color through their chemical structure, cellular localization, and biochemical synthesis pathways. Among these, anthocyanins are key secondary metabolites of flavonoids that can impart red to blue-violet hues to petals. Modifications to anthocyanin, such as methylation, glycosylation, and acylation, can alter petal color[9]. Research has demonstrated that studies on flower color in plants such as *Rosa rugosa*[10], *Dahlia pinnata*[11], and *Nelumbo nucifera*[12] have identified anthocyanins as the primary influencing factor in the coloration of their petals. Variations in the intrinsic pigment content of petals

[1]College of Forestry, Shenyang Agricultural University, Shenyang 110866, Liaoning Province, China. [2]Key Laboratory for Silviculture of Liaoning Province, Shenyang Agricultural University, Shenyang 110866, Liaoning Province, China. [3]Bureau of Forestry and Grassland of Kazuo County, Kazuo, Chaoyang 122300, Liaoning Province, China. ✉email: h910ing@163.com; dsj928@163.com

at different developmental stages can result in differences in extrinsic petal color. One study indicated that in rose flower, increased flavonoids and anthocyanins have caused petal blueing[13]. Physicochemical factors during flowering, such as the activities of enzymes like phenylalaninammo nialyase (PAL) and chalcone isomerase (CHI), the presence of precursors like soluble sugars and proteins, and cytosol pH, indirectly influence flower color by affecting pigment synthesis. Moreover, the epidermal structure of petal cells plays a role in light absorption by pigmented substances, impacting petal color[14]. The epidermal cells of the petal can be categorized into conical and flat cells based on the ratio of their thickness to width. Typically, conical cells enhance the proportion of incident light entering the cells, resulting in greater light absorption and a deeper color of the petal. In contrast, light that strikes the flat cells perpendicularly is predominantly reflected, leading to a lighter coloration of the petal[15]. However, variations exist among different families of plants. In the case of *Phalaenopsis*[16], it was observed that there is no significant correlation between the epidermal structure of the petal cells and the color of the flowers.

To enhance our understanding of the coloring mechanism in pink-flowered *P. sibirica* petals, this research analyzed petals from pink- and white-flowered *P. sibirica* specimens sourced from the National Forest Germplasm Resource Preservation Repository for *Prunus* species at Shenyang Agricultural University (Kazuo, Liaoning, China), and aimed to provide a theoretical basis for new variety cultivation and enriching ecological and ornamental plant resources in northeast China and the northern region. The sampling date and sample size were determined based on preliminary investigations on phenological stages, floral organ traits, and tree traits of pink-flowered *P. sibirica*. In particular, the study focused on measuring and analyzing parameters such as floral color, pigmentation, nutrient content, cytosol pH, and cell morphology during the blossoming process.

Materials and methods

Plant materials

Pink-flowered *P. sibirica* (Appraisal of improved varieties of forest tree, S-SV-PS-001–2023, Liaoning Provincial Department of Forest and Grassland) and white-flowered *P. sibirica* petals (Appraisal of improved varieties of forest tree, S-SC-AS-005–2014, Liaoning Provincial Department of Forest and Grassland) were selected as experimental materials from the National Forest Germplasm Resource Preservation Repository for *Prunus* species at Shenyang Agricultural University (Kazuo, Liaoning, China) (Fig. 1). Each sample, aged 6–7 years with stable genetic traits, was carefully chosen. Three single plants of uniform vigor, robust growth, and free from pests and diseases were selected for each clone. These plants were classified into five stages based on petal color and morphological characteristics: ruddy stage (S1), exposure stage (S2), early flowering stage (S3), blooming stage (S4), and late flowering stage (S5). Petals from each stage were collected between March–April of 2022 and 2023. Some petals were used for observing flower color parameters and anatomical structures, while the remaining petals were promptly frozen in liquid nitrogen and stored at − 80 °C in an ultra-low-temperature refrigerator upon return to the laboratory.

Observation indicators and methods

Determination of color parameters

For the quantitative analysis of the pink- and white-flowered *P. sibirica* petal colors the CIELab color system introduced by the International Commission on Illumination in 1970 was used as a reference [17]. In this study, flower color L^* values (brightness), a^* values (redness), and b^* values (yellowness) were determined by using a colorimeter (CR-10PLUS, Konica minolta/ Japan) aimed at the middle of the petals.

Determination of pigment contents

The flavonoid content of petals was determined using the plant flavonoid test kit from Nanjing Jiancheng Bioengineering Institute. The petals were washed with distilled water, the surface water was wiped dry, ground

Fig. 1. Petals of *P. sibirica* at different stages of blooming. The petals were categorized as: ruddy stage (S1), exposure stage (S2), early flowering stage (S3), blooming stage (S4), and late flowering stage (S5). The top row represents the pink-flowered *P. sibirica* (P1–P5) and the bottom row represents the white-flowered *P. sibirica* (W1–W5). Bar = 5 mm.

to powder in liquid nitrogen, weighed to 0.05 g, 2 mL of extraction solution was added, extracted by shaking at 60 °C for 2 h, 10,000 g, centrifuged at room temperature (around 15 °C) for 10 min, the supernatant was collected and the absorbance measured at 502 nm. Three biological replicates were performed for each developmental stage. The calculation formula was as follows:

$$\text{Flavonoid content } (\text{mg/g}) = \frac{(\Delta A_{502} - 0.0141)}{9.0771 \times V/M}$$

$\triangle A_{502}$, the difference between measurement tube and control tube under 502 nm; V, total volume of the extract (mL); M, sample quality (g).

The anthocyanin, carotenoid, and chlorophyll contents of the petals were determined following the method described by Piccaglia and Scrob [18,19]. Petals were weighed, cut into 0.3 g portions, and placed into two 25 mL stoppered glass test tubes. A mixture of 20 mL of 0.1 mol/L HCl extract and 15 mL of 95% alcohol solution was added to the test tubes, which were then inverted several times to mix. The test tubes were then placed in a thermostat at 32 °C for 16 h and 37 °C for 24 h, respectively. Once all the petals whitened, the test tubes were removed, cooled to room temperature (around 15 °C), and the absorbance was measured at 530 nm using 0.1 mol/L HCl solution as a control. Three biological replicates were performed for each developmental stage. The calculation formula was as follows:

$$\text{Relative content of anthocyanin } (\text{mg/g}) = A_{530}/0.1 \times M$$

A_{530}, the absorbance was measured at 530 nm; M, sample quality (g).

The OD values were determined at 645 nm, 649 nm, and 470 nm using 95% alcohol solution as a control to calculate carotenoid and chlorophyll contents. Three biological replicates were performed for each developmental stage. The calculation formula was as follows:

Chlorophyll a content (mg/g) = $(13.95\ A_{649} - 6.88\ A_{645}) \times V \times N/M$.

Chlorophyll b content (mg/g) = $(24.96\ A_{645} - 7.32\ A_{649}) \times V \times N/M$.

Carotenoid content (mg/g) = $\frac{1000\ A470 - 2.05\ Ca - 114.8\ Cb}{245} \times V \times N/M$.

A, the absorbance were measured at 645 nm, 649 nm, and 470 nm; V, volume of extract (L); N, dilution factor; M, sample quality (g).

Determination of PAL and CHI activities

PAL and CHI activities were assayed using a modified version of the method described by La et al.[20]. PAL activity was determined as follows: for the extraction, 0.5 g of petals were ground in a mortar with 1 mL of 7 mmol/L β-mercaptoethanol, 1 mL of 0.1 mol/L boric acid retardant (containing an appropriate amount of polyvinylpyrrolidone), and 3 mL of the extract solution in an ice bath until homogenized. The mixture was then centrifuged at 12,000 rpm for 15 min at 4 °C, and the supernatant was collected and stored at a low temperature. Subsequently, 5 mL test tubes were prepared by adding 1 mL of 0.02 mol/L phenylalanine, 2 mL of 0.1 mol/L boric acid buffer at pH 8.8, and 0.1 mL of the crude enzyme extract. The contents of each test tube were mixed, and the absorbance at 290 nm was measured using a UV spectrophotometer (U-5100, Hitachi/ Japan). After incubating the tubes in a water bath at 30 °C for 30 min, the absorbance at 290 nm was measured again. The enzyme activity was calculated based on the change in OD value by 0.01 per 30 min, defined as one unit of enzyme activity. Three biological replicates were performed for each developmental stage.

CHI activity was determined as follows: 0.5 g of petals were placed in a mortar and ground with 5 mL of pH 7.0 buffer in an ice bath until homogenized. After which, it was centrifuged at 12,000 rpm for 15 min at 4 °C, and the supernatant was collected and stored at a low temperature. In a 5 mL test tube, 0.1 mL of crude enzyme extract was combined with 0.05 mL of chalcone, and 2.5 mL of bovine serum albumin. The absorbance was measured at 381 nm for 30 min in a water bath at 35 °C. The enzyme activity was calculated based on an increase in OD value of 0.1 per minute, defined as one unit of enzyme activity unit. Three biological replicates were performed for each developmental stage.

Determination of nutrient contents

The soluble sugar content was analyzed following the method described by Liu et al.[21]. Petals weighing 0.5 g were ground and then diluted with 10 mL of distilled water. The mixture was extracted in boiling water for 30 min and then centrifuged at 12,000 rpm for 20 min. The resulting supernatant was collected and diluted to a final volume of 25 mL. Subsequently, 1.5 mL of distilled water, 0.5 mL of ethyl anthrone acetate reagent, and 5 mL of concentrated sulfuric acid were added in sequence. The solution was then placed in a boiling water bath for 1 min after thorough shaking. After cooling to room temperature, the absorbance was measured at 630 nm. Three biological replicates were performed for each developmental stage.

The soluble protein content was assessed using the method described by Kučerová et al.[22]. Petals weighing 0.5 g were ground and then diluted with 10 mL of distilled water. The supernatant was obtained through centrifugation at 10,000 rpm for 15 min. Subsequently, 1 mL of the supernatant was pipetted, mixed with 5 mL of G-250 Coomassie Brilliant Blue solution, allowed to stand for 2 min, and the absorbance at 595 nm was measured. Three biological replicates were performed for each developmental stage.

Determination of cytosol pH

The method described by Zhang et al.[23], with minor adjustments, was utilized to determine the pH of the petal cytosol. Specifically, 0.5 g of petals was ground into a homogenate using a mortar and pestle, with 2 mL of distilled water added during the process. The pH of the resulting homogenate was then measured using a PHS-

3E pH meter (INESA/ China), which served as a proxy for the pH of the petal cytosol. Three biological replicates were performed for each developmental stage.

Observation of petal morphology and structure

Fresh petals were taken after the flowers had fully opened and temporary water mounts were prepared by the freehand sectioning method to observe the upper epidermis of the petals. The mounts were photographed and observed under a light microscope (Primostar 3, ZEISS/ Germany) at 10× magnification.

Paraffin sections were prepared following conventional procedures [5]. The middle portion of the petals was cut and fixed in formaldehyde alcohol acetic acid (FAA) fixative, with section thickness ranging from 6–8 μm. These sections were then stained with Senna solid green and sealed with neutral gum. Observation of the petals was conducted using a light microscope (Olympus-BX51, Hitachi/ Japan), and data analysis was performed using Image J software. Parameters measured included upper epidermal cell thickness, width, thickness-to-width ratio, and cell pinch angle. Three transverse structural sections were obtained from each petal, with 10 fields of view analyzed per section.

Following the methodology outlined by Norikoshi et al.[24], fresh petals were carefully cleaned with distilled water to remove any impurities. Subsequently, 5 mm × 5 mm samples were extracted and immersed in glutaraldehyde fixative for preservation. The petals then underwent a process of gradual dehydration and were dried using a vacuum freeze dryer. These samples were affixed to aluminum trays and coated with gold using an MC1000 ion sputtering instrument before being examined with a Hitachi Regulus 8100 type cold-field emission scanning electron microscope. Epidermal cells on the petals were quantified and analyzed at 500× magnification, with cell morphology observed and captured at 1000× magnification. Data analysis was conducted using Image J software, with measurements repeated nine times for accuracy.

Data analysis

Statistical analysis on all experimental data was completed using SPSS Statistics V 22.0. Results are presented as the mean ± standard deviation (SD), using a significance threshold of $p < 0.05$. The correlation among color parameters, pigment contents, physiological responses, and petal morphology and structure was calculated by Pearson's test at two significance levels, $p < 0.05$ and $p < 0.01$. On the other hand, a stepwise regression analysis at $p < 0.05$ and $p < 0.01$ was done to determine the key factors affecting the petal coloration of pink-flowered *P. sibirica*. Plotting bar charts and heatmaps for correlation analysis were performed using OriginPro 2022 software.

Results

Comparison of color parameters

Pink-flowered *P. sibirica* petals are dark pink at S1, gradually changing to light pink as the flowers open up; whereas, white-flowered *P. sibirica* petals are white from S1 to S5. As shown in Fig. 2, the L^* values of both pink and white petals showed a trend of first increasing and then decreasing. The L^* values of pink petals ranged from 66.73–76.90, while the L^* values of white petals ranged from 71.27–83.87. Notably, the L^* values of pink flower petals were significantly lower than those of white flower petals across all five stages, being 93.64%, 89.28%, 89.51%, 93.40% and 95.64% of the L^* values of white flower petals, respectively. The a^* and L^* values of the petals of the two samples showed an opposite trend, with the a^* values of pink petals ranging from 7.17–16.87, and for white petals from − 1.30 to − 0.50. The a^* values of pink flower petals were significantly higher than those of white flower petals across all five stages, being 33.73, 11.26, 12.36, 8.96, and 12.48 times higher, respectively. The b^* values of both pink and white flowers showed a gradually increasing trend, with the b^* values of pink flowers ranging from 2.33 to 8.07 and those of white flowers from 8.67 to 12.90. In all stages of flowering, the b^* values of pink flower petals were significantly lower than those of white flower petals.

Comparison of pigment contents

As shown in Table 1, the anthocyanin and total chlorophyll contents of both pink and white flower petals showed a trend of initially increasing and then decreasing, with the maximum values of anthocyanin and total chlorophyll of pink flower petals observed at S2, respectively. The chlorophyll a and chlorophyll b contents of pink flower petals reached a maximum at S2, whereas the chlorophyll a and chlorophyll b contents of white flower petals reached a maximum at S3 and S4, respectively. The anthocyanin content of pink flower petals increased by 25.84% at S2 compared to the beginning and decreased to 2.22 mg/g at S5, which was 62.18% lower compared to S1. Across all five stages, the anthocyanin content of pink flower petals was significantly higher than that of white flower petals. In the pre-flowering stage, the total chlorophyll content of pink flower petals was significantly higher than that of white flower petals. However, no significant difference was observed between the total chlorophyll content of pink and white flower petals at S4 and S5.

The flavonoid and carotenoid content of both pink and white flowers showed a decreasing trend, the flavonoid and carotenoid contents of pink petals decreased by 64.23% and 77.33%, respectively, at S5 compared to S1. Similarly, the flavonoid and carotenoid contents of white petals decreased by 80.23% and 70.51%, respectively, at S5 relative to S1. Notably, the flavonoid content and carotenoid content of pink petals were significantly higher than those of white petals at all five stages.

Comparison of PAL and CHI activities

As shown in Table 2, the PAL activities of both pink and white petals displayed a pattern characterized by an initial increase followed by a subsequent decrease. The highest activities were recorded at S2, reaching 29.69 U/g for pink petals and 8.39 U/g for white petals. The PAL activity decreased by 85.08% for pink petals and 68.65% for white petals during the S5, compared to S2. The PAL activity of pink flower petals was significantly higher than that of white flower petals, being 7.57, 3.54, 3.07, and 2.19 times higher at S1, S2, S3, and S4, respectively.

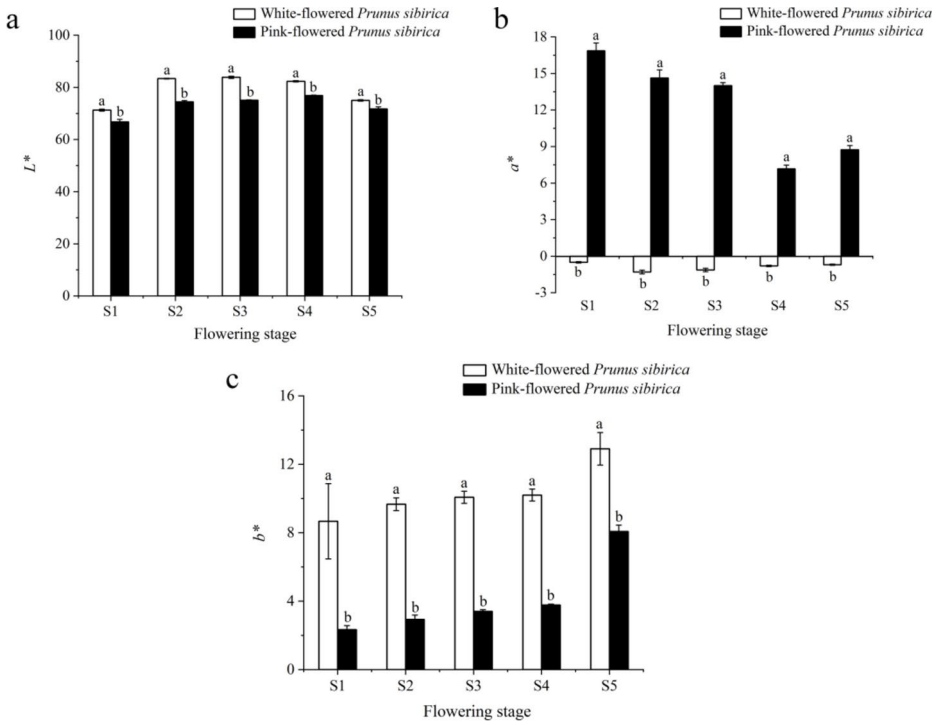

Fig. 2. Comparison of color parameters in pink- and white-flowered *P. sibirica*. The comparison of the lightness (L^* values) of the two samples (**a**), the comparison of the redness (a^* values) of the two samples (**b**), and the comparison of the yellowness (b^* values) of the two samples (**c**). Different lowercase letters indicate significant differences at the $p < 0.05$ level, the same letter means no significant difference. Error bars represent standard deviation.

Flowering stage	Samples	Flavonoid (mg/g)	Anthocyanins (mg/g)	Carotenoid (mg/g)	Chlorophyll (mg/g)	Chlorophyll a (mg/g)	Chlorophyll b (mg/g)
S1	P	16.02 ± 1.75 a	5.87 ± 0.06 a	2.25 ± 0.01 a	0.44 ± 0.01 a	0.18 ± 0.03 a	0.26 ± 0.01 a
	W	7.84 ± 2.52 b	0.16 ± 0.01 b	1.56 ± 0.10 b	0.30 ± 0.01 b	0.11 ± 0.01 b	0.17 ± 0.01 b
S2	P	7.92 ± 0.07 a	7.39 ± 0.30 a	1.23 ± 0.16 a	1.81 ± 0.04 a	0.72 ± 0.08 a	1.09 ± 0.07 a
	W	5.28 ± 0.49 b	0.75 ± 0.02 b	0.92 ± 0.06 b	0.77 ± 0.10 b	0.31 ± 0.08 b	0.46 ± 0.08 b
S3	P	6.92 ± 1.21a	6.52 ± 0.04 a	0.96 ± 0.15 a	1.02 ± 0.04 a	0.34 ± 0.10 a	0.68 ± 0.15 a
	W	3.40 ± 0.75 b	0.65 ± 0.02 b	0.88 ± 0.08 a	0.79 ± 0.09 b	0.33 ± 0.07 a	0.46 ± 0.03 b
S4	P	6.75 ± 0.35 a	5.17 ± 0.03 a	0.93 ± 0.04 a	1.00 ± 0.06 a	0.40 ± 0.14 a	0.60 ± 0.10 a
	W	3.30 ± 0.46 b	0.59 ± 0.08 b	0.50 ± 0.13 b	0.88 ± 0.06 a	0.29 ± 0.05 a	0.59 ± 0.04 a
S5	P	5.73 ± 0.27 a	2.22 ± 0.18 a	0.51 ± 0.04 a	0.38 ± 0.10 a	0.11 ± 0.03 a	0.27 ± 0.07 a
	W	1.55 ± 0.24 b	0.51 ± 0.06 b	0.46 ± 0.05 a	0.33 ± 0.01 a	0.07 ± 0.04 a	0.26 ± 0.04 a

Table 1. Comparison of petal pigments in different *Prunus sibirica* samples. Different lowercase letters within the same column indicate significant differences at the 0.05 levels between petals at the same time stage. P: Pink-flowered *P. sibirica*; W: White-flowered *P. sibirica*.

The CHI activities of both pink and white flower petals showed a gradually decreasing trend. The CHI activities decreased by 79.00% and 68.15% at S5 of pink and white petals, respectively, compared to S1. The CHI activity of pink flower petals was significantly higher than that of white flower petals across all five stages, being 2.10, 2.02, 2.20, 1.70, and 1.39 times higher, respectively.

Comparison of nutrient contents and cytosol pH

As shown in Table 3, the soluble sugar content of both pink and white petals showed a trend of initially increasing followed by then decreasing. The highest content of 35.28 mg/g and 32.54 mg/g was observed at S2 and S4 for pink and white petals, respectively. The soluble sugar content of pink petals increased by 7.07% at S2 but decreased by 11.23% at S5 when compared to the S1. In contrast, the soluble sugar content of white petals decreased by 4.56% at S5 relative to the S1. The soluble sugar content of pink flower petals was significantly higher than that of white flower petals, being 1.06, 1.10 and 1.06 times higher at S1, S2 and S4, respectively. The trend of the soluble protein content of pink and white petals was different, with pink petals exhibiting a

Flowering stage	Samples	PAL activity (U/g)	CHI activity (U/g)
S1	P	14.95 ± 1.14 a	46.67 ± 1.03 a
	W	1.97 ± 0.07 b	22.20 ± 1.25 b
S2	P	29.69 ± 1.14 a	34.87 ± 1.47 a
	W	8.39 ± 1.18 b	17.27 ± 0.81 b
S3	P	21.80 ± 2.31 a	21.13 ± 1.63 a
	W	7.09 ± 0.90 b	9.60 ± 0.87 b
S4	P	8.76 ± 0.89 a	13.47 ± 2.10 a
	W	3.99 ± 0.36 b	7.93 ± 0.12 b
S5	P	4.43 ± 1.14 a	9.80 ± 0.35 a
	W	2.63 ± 1.03 a	7.07 ± 0.12 b

Table 2. Comparison of petal PAL and CHI activities in different *Prunus sibirica* samples. Different lowercase letters within the same column indicate significant differences at the 0.05 levels between petals at the same time stage. P: pink-flowered *P. sibirica*; W: white-flowered *P. sibirica.*

Flowering stage	Samples	Soluble sugar (mg/g)	Soluble protein (mg/g)	Cytosol pH
S1	P	32.95 ± 0.40 a	6.02 ± 12.32 b	5.14 ± 0.02 b
	W	31.14 ± 0.38 b	12.32 ± 0.27 a	5.28 ± 0.05 a
S2	P	35.28 ± 0.17 a	4.85 ± 0.18 b	5.17 ± 0.06 b
	W	32.01 ± 0.07 b	12.92 ± 0.13 a	5.51 ± 0.06 a
S3	P	34.63 ± 0.42 a	3.54 ± 0.04 b	5.18 ± 0.05 b
	W	32.12 ± 3.28 a	19.86 ± 0.27 a	5.52 ± 0.12 a
S4	P	34.53 ± 0.37 a	6.80 ± 0.31 b	5.24 ± 0.02 b
	W	32.54 ± 0.05 b	29.04 ± 0.72 a	5.55 ± 0.12 a
S5	P	29.25 ± 0.49 a	9.32 ± 0.10 b	5.45 ± 0.02 b
	W	29.72 ± 1.12 a	25.33 ± 0.31 a	6.16 ± 0.09 a

Table 3. Comparison of petal soluble sugars, soluble protein content, and cytosol pH in different *Prunus sibirica* samples. Different lowercase letters within the same column indicate significant differences at the 0.05 levels between petals at the same time stage. P: pink-flowered *P. sibirica*; W: white-flowered *P. sibirica.*

pattern of first decreasing and then increasing, while white petals showed the opposite trend of increasing and then decreasing. The soluble protein content of the petals of pink and white flowers reached maximum values of 9.32 mg/g and 29.04 mg/g at S5 and S4, respectively. At S5, the soluble protein content was elevated by 54.82% and 105.60% in pink and white petals, respectively, compared to the S1. The soluble protein content within the petals of pink flowers was significantly lower than that of white flowers across all five stages, being 48.86%, 37.54%, 17.82%, 23.42%, and 36.79% of that of white flower petals, respectively. The cytosol pH of the petals of both pink and white flowers showed a gradual increase. Furthermore, across all five stages, the cytosol pH of pink flower petals was significantly lower than that of white flower petals, being 97.35%, 93.83%, 93.90%, 94.36% and 88.47% of that of white flower petals, respectively.

Comparison of the internal microstructure of petals

Observations on the upper epidermis of fully open petals by freehand sectioning revealed differences in epidermal cell morphology and pigment distribution among different colored petals (Fig. 3). The epidermal cell structure on the petals of pink flowers appeared irregularly shaped, accompanied by conspicuous pigment distribution (Fig. 3a). It was hypothesized the majority of these pigments might be anthocyanins. Conversely, the epidermal cell structure on the petals of white flowers exhibited nearly rectangular shapes, devoid of obvious pigment accumulation (Fig. 3b).

The use of paraffin sectioning experiments allowed for better observation of changes in petal sections (Fig. 4). The upper epidermal cell thickness and width of both pink and white flowers petals exhibited an initial increase followed by a subsequent decrease (Fig. 6a and b). Additionally, the thickness-to-width ratio of epidermal cells on petals is representative of the degree of conicity of the cells. During the flowering process, the thickness-to-width ratios of the epidermal cells on the petals of both pink and white flowers displayed a trend of decreasing initially, followed by an increase (Fig. 6c). The highest values of the thickness-to-width ratios of the epidermal cells on the petals of both pink and white flowers were found at S1, while the lowest values were found at S4. At S2, the thickness-to-width ratios of the epidermal cells on the petals of pink flowers were significantly higher than those on the petals of white flowers, being 1.20 times as high as those on white flowers. Conversely, at S3, the thickness-to-width ratios of the epidermal cells on the petals of pink flowers were significantly lower than those on the petals of white flowers, accounting for only 79.26% of those on white flowers.

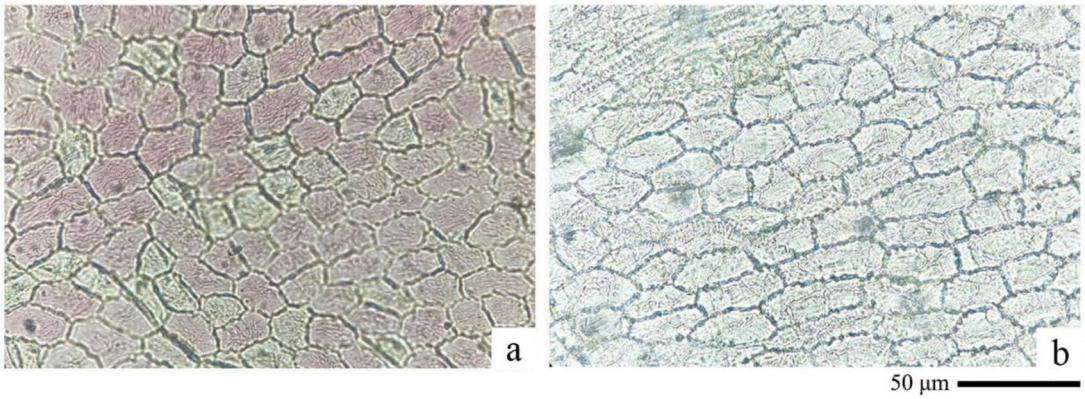

Fig. 3. Morphology and pigment distribution of the upper epidermis of the petals of pink-flowered *P. sibirica* (**a**), morphology and pigment distribution of the upper epidermis of the petals of white-flowered *P. sibirica* (**b**).

The epidermal cell angle on the petals of both pink and white flowers followed a similar pattern, initially increasing and then decreasing (Fig. 6d). In particular, the epidermal cell angle on the petals of both pink and white flowers was the largest at S4 and the smallest at S1. At S1, the angle of the epidermal cells on the petals of pink flowers was significantly lower than that on the petals of white flowers, accounting for only 54.84% of the petals of white flowers. However, at S3 and S5, the angle of the epidermal cells on the petals of pink flowers was significantly higher than that on the petals of white flowers, being 1.08 and 1.14 times as high as that on the petals of white flowers.

Scanning electron microscope images showed changes in the upper epidermal cells of the petals of *P. sibirica* at five stages (Fig. 5). Noticeable trends in the epidermal cell area on the petals of pink flowers showed a trend of increasing and then decreasing, whereas the number of cells per unit showed a continuous downward trend. Conversely, the epidermal cell area on the petals of white flowers showed a gradual upward trend, and the number of cells per unit showed a trend of initially decreasing followed by increasing (Fig. 6e and f). At S1, the area of epidermal cells on pink flower petals was significantly lower than that on white flower petals, accounting for 83.62% of that on white flower petals. The number of epidermal cells on the petals of pink flowers was significantly higher than that on the petals of white flowers at S1, S2 and S4, being 1.54 1.61 and 1.13 times higher, respectively. Additionally, at S5, the number of epidermal cells on the petals of pink flowers was significantly lower than that on the petals of white flowers, being 79.73% lower than that of the petals of white flowers.

Comprehensive analysis among indicators

Pearson's correlation matrix showed the correlation between the different variables (Fig. 7), pink flower petal L^* values were significantly negatively correlated with a^* values ($p < 0.05$). However, there was no significant correlation between L^* values and b^* values. However, a^* values were significantly negatively correlated with b^* values. Furthermore, the L^* values showed highly significant positive correlations ($p < 0.01$) with upper epidermal cell width, cell pinch angle, and cell area, and significant positive correlations with total chlorophyll and chlorophyll b content. The L^* values showed highly significant negative correlations with flavonoid content, carotenoid content, upper epidermal cell thickness to width ratio and cell number, and significant negative correlations with CHI activity. Furthermore, the a^* values showed a highly significant positive correlation with flavonoid content, carotenoid content, PAL activity, CHI activity, the thickness-to-width ratio of upper epidermal cells and cell number, and a significant positive correlation with anthocyanin content. Conversely, a highly significant negative correlation with cytosol pH, upper epidermal cell pinch angle and cell area, and significant negative correlation with soluble protein content. In addition, The b^* values showed highly significant positive correlations with soluble protein and cytosol pH, significant positive correlations with upper epidermal cell pinch angle and cell area. In contrast, b^* values showed highly significant negative correlations with anthocyanin content, carotenoid content, PAL activity, CHI activity, soluble sugar content and upper epidermal cell thickness, and significant negative correlation with flavonoid content and upper epidermal cell number.

As shown in Table 4, the insignificant independent variables were excluded at the 5% significant level, and the indicators with partial regression coefficients reaching significant or highly significant levels were selected to enter into the regression equation for flower color, and the indicators with the most significant effects on the a^* and b^* values of petal were further found from each indicator significantly correlated with flower color. In the stepwise regression equation for the a^* value of pink petals, four indicators, namely anthocyanin content, CHI activity, upper epidermal cell area and soluble proteins, were retained and all the rest were excluded. In the stepwise regression equation for the b^* value, two indicators, namely anthocyanin content and PAL activity, were retained and all the rest were excluded. This result suggests that anthocyanins play an important role in the colouration of the petals of pink-flowered *P. sibirica*.

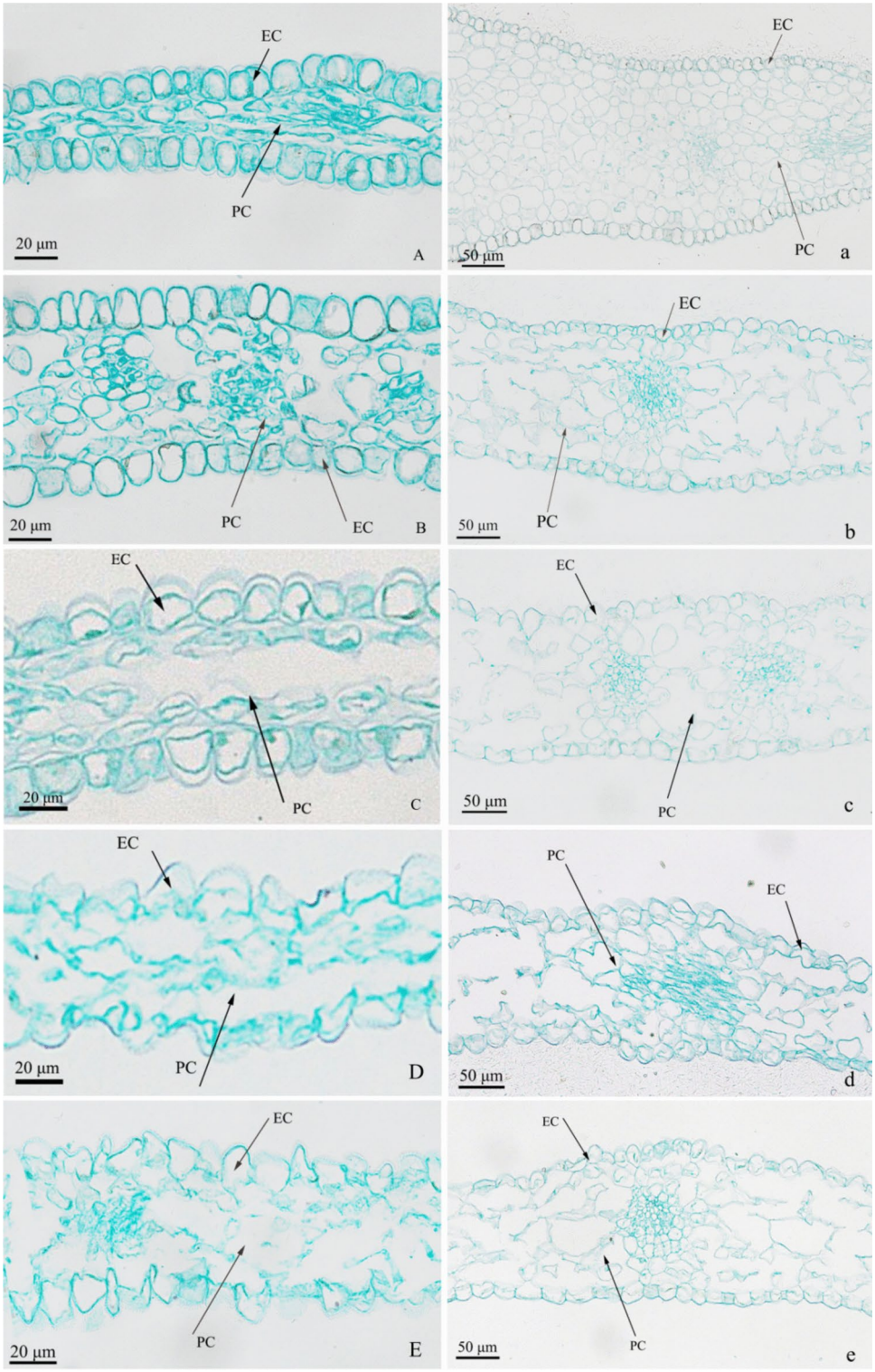

Fig. 4. Capital letters represent the cross-sectioned structure of the pink-flowered *P. sibirica* petals, lowercase letters represent the cross-sectioned structure of the white-flowered *P. sibirica* petals; (**A** & **a**) ruddy stage; (**B** & **b**) exposure stage; (**C** & **c**) early flowering stage; (**D** & **d**) blooming stage; (**E** & **e**) late flowering stage; EC: epidermal cell; PC: parenchyma cell.

Discussion

Flower color is an important feature of ornamental plants, and the determination of flower color parameters to further explore the mechanism of flower color formation has been widely used in plants such as *Rhododendron*[25], Snapdragon[26], and *Lagerstroemia*[27]. The CIELab system is a commonly used method for determining the

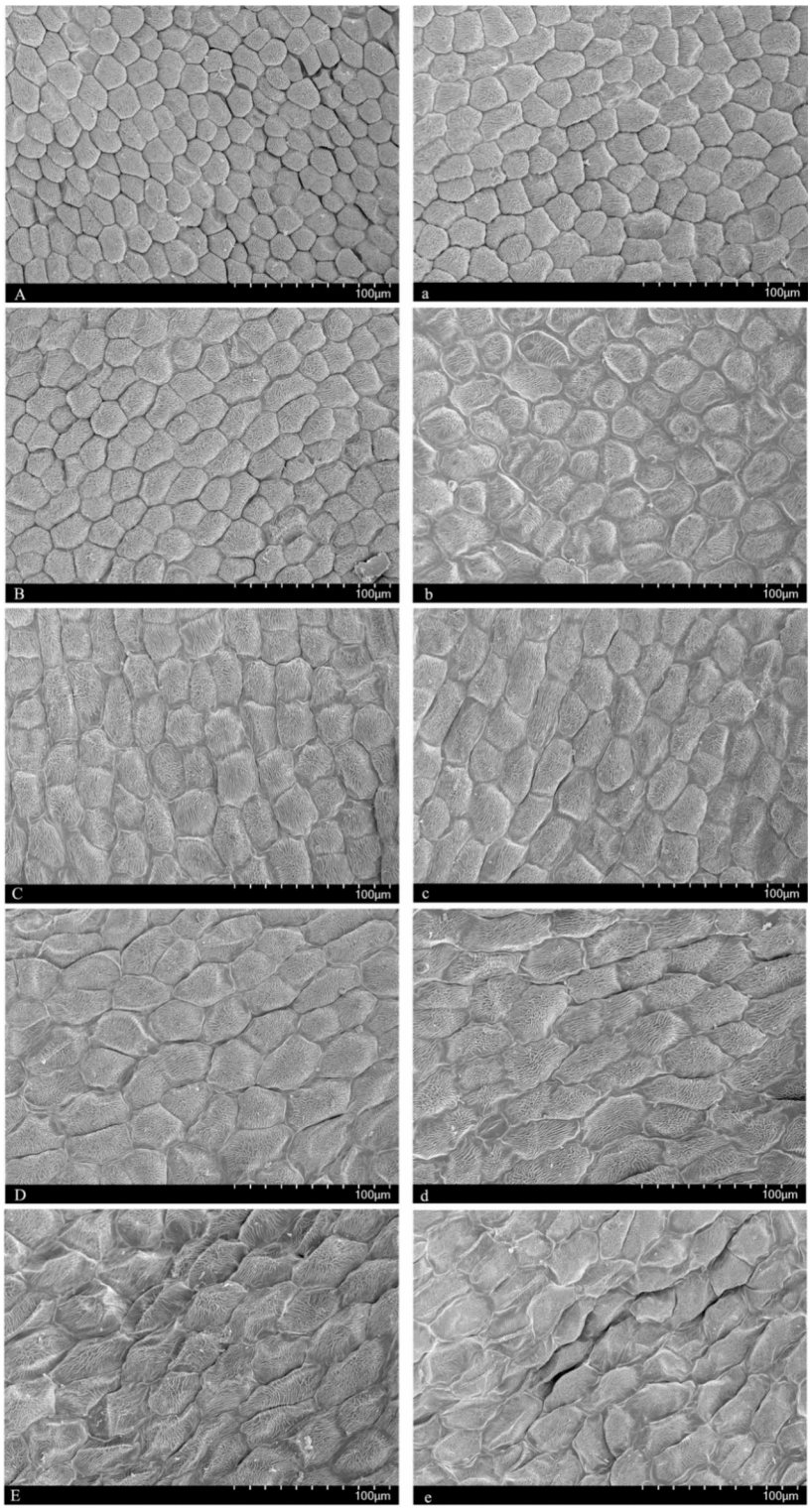

Fig. 5. Morphology of the epidermal cells on the petals of *P. sibirica* at different stages of blooming. (**A**–**E**) are pink-flowered *P. sibirica* petals, (**a**–**e**) are white-flowered *P. sibirica* petals. All images are petal morphology at 500× magnification.

parameters of flower color as it quantifies the brightness, redness, and yellowness of the petals through the use of the L^* value, the a^* value, and the b^* value, respectively[28]. Changes in the L^* values, the a^* values and the b^* values during the opening process of *P. sibirica* flowers indicate that petals gradually unfolded, petals become increasingly pale. The L^* and b^* values of pink petals were significantly lower than those of white petals, and the a^* value was significantly higher than that of white petals, which visually reflected that the color of pink petals

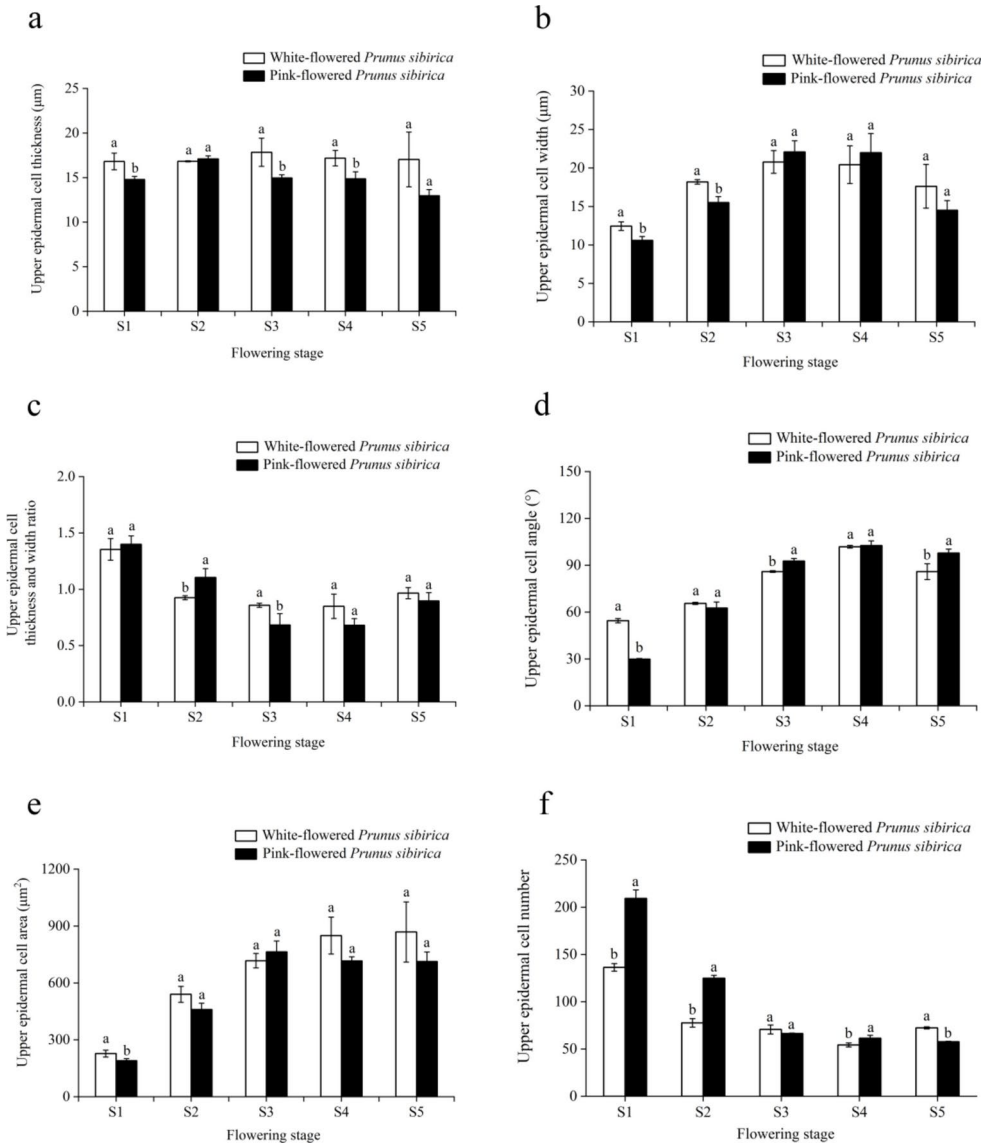

Fig. 6. Comparison of multiple comparisons of quantitative parameters of epidermal cells in pink- and white-flowered *P. sibirica*. The comparison of the upper epidermal cell thickness of the two samples (**a**), the comparison of the upper epidermal cell width of the two samples (**b**), the comparison of the upper epidermal cell thickness and width ratio of the two samples (**c**), the comparison of the upper epidermal cell angle of the two samples (**d**), the comparison of the upper epidermal cell area of the two samples (**e**), and the comparison of the upper epidermal cell number of the two samples (**f**).

was more intense than that of white petals at different stages of time. This indicates that the CIELab system was able to capture and quantify the subtle changes in petal color effectively to provide us with an accurate picture of the changes in flower color[29]. In this study, the L^* values of the petals were negatively correlated with the a^* values and not significantly correlated with the b^* values. Notably, pink flowers from *P. sibirica* varieties are better evaluated based on a^* values rather than b^* values for their color assessment.

The type and concentration of pigments in the petals are the main factors affecting the petal coloration, with anthocyanins predominantly regulating the pink to blue-violet color of the petals[30,31].

In our study, correlation and stepwise regression analyses together showed that anthocyanins play an important role in pink-flowered *P. sibirica* petal coloration. We observed that the pink flower petals were not fully unfolded and had a dark color during the pre-flowering stage. The anthocyanin content peaked during the exposure stage, suggesting complete accumulation during the pre-flowering stage. A strong positive relationship between the a^* value of pink flower petals and anthocyanin content, indicating that changes in anthocyanin levels directly impacted the color intensity of pink flower petals at various stages[13]. Building on previous research[32,33], future studies could employ high-performance liquid chromatography-mass spectrometry (HPLC–MS) for the quantitative analysis of anthocyanins in pink-flowered *P. sibirica*. This approach could help identify unique compounds in *P. sibirica* flower petals at a secondary metabolism level, shedding light on the

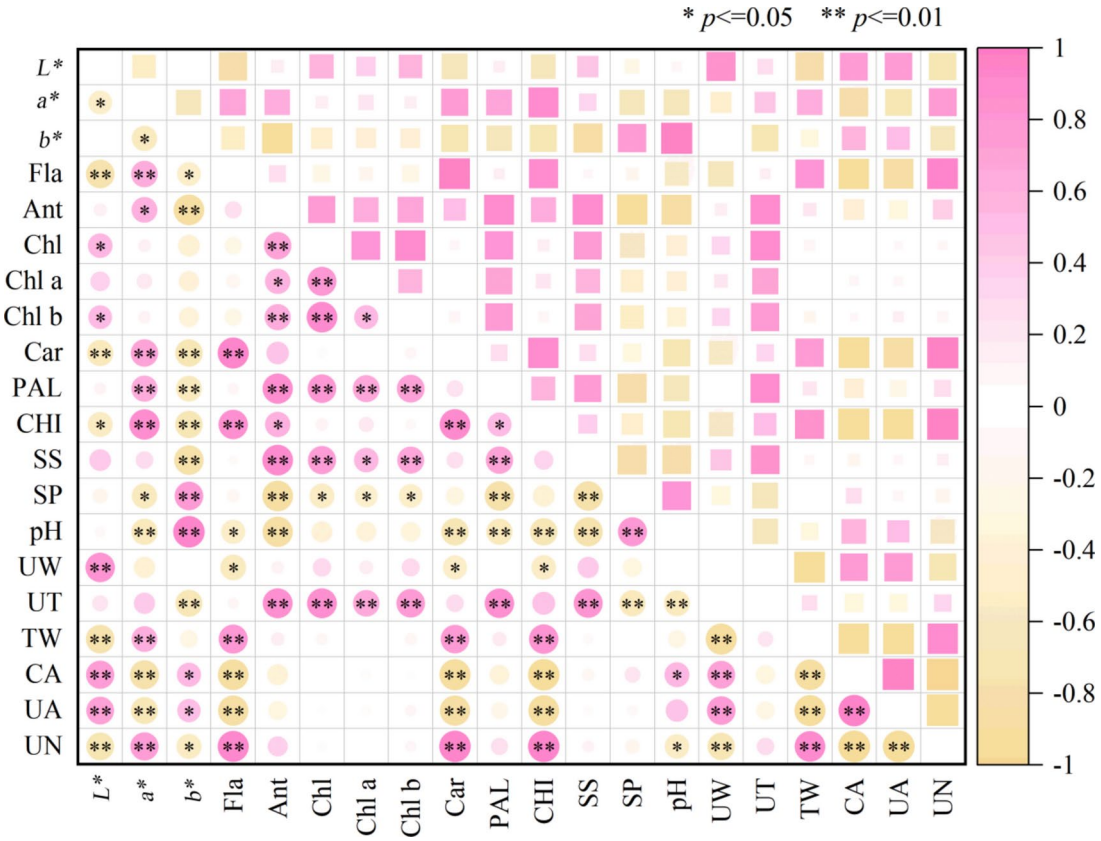

Fig. 7. Correlation coefficients among the indicators of petals of pink-flowered *P. sibirica*. Fla. Flavonoid content; Ant. Anthocyanin content; Chl. Total chlorophyll content; Chl a. Chlorophyll a content; Chl b. Chlorophyll b content; Car. Carotenoid content; SS. Soluble sugar content; SP. Soluble protein content; PT. Petal thickness; UT. Upper epidermal thickness; UW. Upper epidermal width; TW. Thickness and width ratio; CA. Upper epidermal cell angle; UA. Upper epidermal cell area; NU. Upper epidermal cell number.

Color parameters	Stepwise regression equation	*F* value	Multiple correlation coefficient
*a**	$y = -1.058A + 0.269B + 0.001C - 1.368D + 18.3$	86.958	0.972
*b**	$y = -1.793A + 0.162E + 11.262$	82.506	0.932

Table 4. Stepwise regression for flower color parameters of pink-flowered *P. sibirica* with various indicators. *A* refers to anthocyanin; *B* refers to CHI activity; *C* refers to upper epidermal cell area; *D* refers to soluble protein; *E* refers to PAL activity.

pigment metabolism mechanism. The flavonoid and carotenoid contents of pink petals were highly significantly and positively correlated with the a^* value, and changes in their contents to some extent aided the colouring of pink petals. The accumulation of large amounts of chlorophyll can mask the color of petals[34], but the chlorophyll content in this study is lower than the other pigments and there is no significant correlation with the a^* value.

The synthesis of anthocyanin, a key pigment influencing the color of pink flower petals, initiates with phenylalanine and involves various enzymes along the metabolic pathway. Notably, PAL and CHI act as upstream synthetases and play a crucial role in anthocyanin production, thereby impacting flower color expression[35]. The findings from previous studies regarding the influence of individual enzymes on anthocyanin synthesis have yielded varied conclusions. For instance, in the examination of the coloration of *Nymphaea hybrid*[36], it was determined that PAL and CHI were extremely important for anthocyanin synthesis. Conversely, in the study on the coloration of *Litchi*'s pericarp[37], it was determined that neither PAL nor CHI exhibited a significant correlation with anthocyanin synthesis, indicating that CHI was not closely related to anthocyanin synthesis. In this study, the anthocyanin content of pink flower petals showed a highly significant and significant positive correlation with PAL and CHI activities, respectively, and the a^* values showed a highly significant positive correlation with the changes in the activities of both. These finding suggest that PAL and CHI activities both affect anthocyanin synthesis and hence flower color changes.

Sugars, as precursors of anthocyanin synthesis, can influence the synthesis of anthocyanins. In addition, soluble sugars, together with soluble proteins, serve as an important source of energy for the vital activities of

petals[38,39]. In this study, there was a highly significant positive correlation between the content of soluble sugars and anthocyanins within the petals of pink flowers, indicating that the accumulation of soluble sugars promoted the production of anthocyanins. However, there was no significant correlation between the soluble sugar content and the a^* value, indicating that soluble sugars are not a direct factor influencing petal coloration. The soluble protein content of pink flower petals and white flower petals exhibited opposite trends across the different stages of blooming, while the anthocyanin content remained consistent. In pink flower petals, the soluble protein content showed a highly significant negative correlation with the anthocyanin content. Although some studies have shown that an increase in the soluble protein content inhibits anthocyanin synthesis[40], this conclusion may be applicable mainly to species that are rich in anthocyanins. The extent to which soluble proteins influence anthocyanins synthesis needs to be further explored to fully understand their role across various species and conditions.

Numerous studies have shown that petals tend to be more red in color and anthocyanins can exist more stably when the pH of the petal cytosol is low, and more blue when the pH is high[41]. In this study, the cytosol pH of pink and white flower petals was weakly acidic at all stages of blooming, which was favorable for the preservation and accumulation of anthocyanins. In the correlation analysis, as the pH value of the cytosol increased, anthocyanins gradually degraded, and the color of pink flower petals gradually became lighter. This finding aligns with the results of a study on the mechanism of color presentation in *Hibiscus sabdariffa* L.[42].

Petals are the carriers of flower color, and in this study, significant epidermal pigment accumulation was on the petals of pink flowers, while no significant pigment accumulation was noted on the epidermis of the petals of white flowers using the freehand sectioning method. This suggests that the presentation of the color of the white flowers is not due to pigmentation but is instead an optical phenomenon[41,43]. A variety of flowers, such as the white-flowered *P. sibirica*, take on a white hue due to the presence of numerous air bubbles within their petals, which causes incident light to enter the petals and refract multiple times.

After observing the cross-section structure of petals using the paraffin section method, we found that the epidermal cells of the petals of pink and white flowers were closely arranged and regular in shape during the early stage of flowering. As the petals gradually unfolded, the epidermal cells appeared to be fragmented, and the thin-walled tissues became gradually loosened. The epidermal cells of both the flower types exhibited similar structural changes. It was hypothesized that the differences in the content and distribution of pigments influence the light-absorbing characteristics of the petals, leading to the color differences between the petals of the pink flowers and white flowers[15]. The ratio of epidermal cell thickness and width to the angle of cell entrapment is commonly used to evaluate the degree of canonicalization of cells[44]. Correlation analysis indicates that the higher the degree of canonicalization of the epidermis of the powdered flower petals, the smaller the angle of the intercellular pinch, and the higher the proportion of incident light entering the epidermal cells, which could enhance the absorption of light by the epidermal pigments, thus resulting in denser colors of the petals[45].

Observation of petal epidermal cells by scanning electron microscopy revealed that variations in the area of petal epidermal cells and the number of cells per unit affect the petal color[46,47]. In this study, the a^* value showed a highly significant negative correlation with the area of the upper epidermal cells of the petals and a highly significant positive correlation with the number of upper epidermal cells. This suggests that the rapid expansion of the petal area would result in a corresponding reduction in the number of cells per unit area, but the rate of pigment synthesis would be relatively slow, reducing the pigment content per unit area and resulting in a lighter petal color[47].

During the dissection of petals at each stage of flowering, thinner petals were difficult to observe by freehand sectioning treatment due to variations in petal thickness. To explore the relationship between petal microstructure and coloration, this study used paraffin sectioning and scanning electron microscopy for the multi-dimensional observation of petal transverse structure and petal epidermal cells across the five different stages of flowering. We hope that this comprehensive approach will serve as a useful reference for future researchers.

Conclusion

In this study, we measured the flower color parameters and physiological indicators of pink-flowered and white-flowered *P. sibirica* petals, observed the changes in epidermal cells, and interpreted the mechanism of pink-flowered *P. sibirica* petal coloration from multiple perspectives. The results showed that the a^* value is the primary flower color parameter describing pink-flowered *P. sibirica* petals, with anthocyanins being the main pigments influencing this value. The elevation of PAL and CHI activities, along with soluble sugar content, promoted the synthesis and accumulation of anthocyanins. During this process, the soluble protein content and cytosol pH were lower, and these parameters influenced the anthocyanin content by participating in the physiological processes related to petal coloring, indirectly affecting petal color changes. The thickness-to-width ratio, cell pinch angle, cell area, and number of cells in the upper epidermal of pink flower petals influenced the absorption of light by the petal pigments, resulting in different petal colors at different stages. The results of this study offer an initial insight into the mechanism underlying the coloration of pink-flowered *P. sibirica*, providing a foundation for future studies to delve deeper into the petal color genetics, transcription factors, and other regulatory mechanisms, to comprehensively analyze the formation and regulation of flower color in pink-flowered *P. sibirica* flower, and to provide a theoretical basis for the cultivation of new varieties of ornamental plant varieties with desired flower colors.

Data availability

The datasets generated during and analyzed during the current study are available from the corresponding author on reasonable request.

Received: 12 December 2024; Accepted: 19 February 2025
Published online: 28 February 2025

References

1. Ma, Y. X. et al. Oil content, fatty acid composition and biodiesel properties among natural provenances of Siberian apricot (Prunus sibirica L.) from China. *GCB Bioenergy* **13**, 112–132. https://doi.org/10.1111/gcbb.12759 (2021).
2. Zhao, G. L., Liu, M. G., Dong, S. J. & Liu, Q. H. Specific germplasm of *Prunus Sibirica* in Chaoyang Liaoning. *China Fruits.* **02**, 27–29+81. https://doi.org/10.16626/j.cnki.issn1000-8047.2008.02.014 (2008).
3. Liu, Q. G. et al. Genome-wide identification and analysis of the WRKY gene family and low-temperature stress response in *Prunus sibirica*. *BMC Genomics* **24**, 358. https://doi.org/10.1186/s12864-023-09469-0 (2023).
4. Wang, Z. et al. Comparative transcriptome analysis identifies differentially expressed genes between normal and late-blooming Siberian apricot. *J. For. Res.* **30**, 2277–2288. https://doi.org/10.1007/s11676-018-0825-0 (2018).
5. Chen, J. H. et al. Physiological characteristics of pistil abortion in *Prunus sibirica*. *Trees* **38**, 655–666. https://doi.org/10.1007/s00468-024-02504-x (2024).
6. Zhao, D. Q. & Tao, J. Recent advances on the development and regulation of flower color in ornamental plants. *Front. Plant Sci.* **6**, 125534. https://doi.org/10.3389/fpls.2015.00261 (2015).
7. Ai, Y. et al. Molecular mechanism of different flower color formation of Cymbidium ensifolium. *Plant Mol. Biol.* **113**, 193–204. https://doi.org/10.1007/s11103-023-01382-0 (2023).
8. Tanaka, Y., Tsuda, S. & Kusumi, T. Metabolic engineering to modify flower color. *Plant Cell Physiol.* **39**, 1119–1126. https://doi.org/10.1093/oxfordjournals.pcp.a029312 (1998).
9. Matsuba, Y. et al. A novel glucosylation reaction on anthocyanins catalyzed by acyl-glucose-dependent glucosyltransferase in the petals of carnation and delphinium. *Plant Cell* **22**, 3374–3389. https://doi.org/10.1105/tpc.110.077487 (2010).
10. Zan, W. X. et al. Analysis of flower color diversity revealed the co-regulation of cyanidin and peonidin in the red petals coloration of *Rosa rugosa*. *Plant Physiol. Biochem.* **216**, 109126. https://doi.org/10.1016/j.plaphy.2024.109126 (2024).
11. Granados-Balbuena, S. Y. et al. Identification of anthocyanic profile and determination of antioxidant activity of *Dahlia pinnata* petals: A potential source of anthocyanins. *J. Food Sci.* **87**, 957–967. https://doi.org/10.1111/1750-3841.16072 (2022).
12. Liu, J. et al. Color fading in lotus (*Nelumbo nucifera*) petals is manipulated both by anthocyanin biosynthesis reduction and active degradation. *Plant Physiol. Biochem.* **179**, 100–107. https://doi.org/10.1016/j.plaphy.2022.03.021 (2022).
13. Schmitzer, V., Veberic, R., Osterc, G. & Stampar, F. Color and phenolic content changes during flower development in groundcover rose. *JASHS* **135**, 195–202. https://doi.org/10.21273/JASHS.135.3.195 (2010).
14. Zhao, D. Q., Wei, M. R., Liu, D. & Tao, J. Anatomical and biochemical analysis reveal the role of anthocyanins in flower coloration of herbaceous peony. *Plant Physiol Biochem.* **102**, 97–106. https://doi.org/10.1016/j.plaphy.2016.02.023 (2016).
15. Zhang, X. P., Zhao, M. Y., Guo, J., Zhao, L. Y. & Xu, Z. D. Anatomical and biochemical analyses reveal the mechanism of double-color formation in *Paeonia suffruticosa* "Shima Nishiki". *3 Biotech* **8**, 1–9. https://doi.org/10.1007/s13205-018-1459-9 (2018).
16. Xiao, W. F., Li, Z., Chen, H. M. & Lv, F. B. Comparing the petal microstructure of different color *Phalaenopsis*. *Chinese Agricult. Sci. Bull.* **33**, 104–111 (2017).
17. Milla´n, M. S. Color pattern recognition with CIELAB coordinates. *Opt. Eng.* **41**, 130–138. https://doi.org/10.1117/1.1428295 (2002).
18. Piccaglia, R., Marotti, M. & Baldoni, G. Factors influencing anthocyanin content in red cabbage (*Brassica oleracea* var *capitata* L f rubra (L) Thell). *J. Sci. Food Agric.* **82**, 1504–1509. https://doi.org/10.1002/jsfa.1226 (2002).
19. Scrob, T., Hosu, A. & Cimpoiu, C. The influence of in vitro gastrointestinal digestion of *Brassica oleracea* florets on the antioxidant activity and chlorophyll, carotenoid and phenolic content. *Antioxidants* **8**, 212. https://doi.org/10.3390/antiox8070212 (2019).
20. La, V. H. et al. Drought stress-responsive abscisic acid and salicylic acid crosstalk with the phenylpropanoid pathway in soybean seeds. *Physiol Plant.* **175**(5), e14050. https://doi.org/10.1111/ppl.14050 (2023).
21. Liu, M. X., Xu, Z. G., Yang, Y. & Feng, Y. J. Effects of different spectral lights on Oncidium PLBs induction, proliferation, and plant regeneration. *Plant Cell Tissue Organ Cult. (PCTOC).* **106**, 1–10. https://doi.org/10.1007/s11240-010-9887-1 (2010).
22. Kučerová, K., Henselová, M., Slováková, Ľ & Hensel, K. Effects of plasma activated water on wheat: Germination, growth parameters, photosynthetic pigments, soluble protein content, and antioxidant enzymes activity. *Plasma Processes Polym.* **16**, 1800131. https://doi.org/10.1002/ppap.201800131 (2019).
23. Zhang, D. L. et al. Analysis of physiological and biochemical factors affecting flower color of Herbaceous Peony in different flowering periods. *Horticulturae* **9**, 502. https://doi.org/10.3390/horticulturae9040502 (2023).
24. Norikoshi, R., Shibata, T. & Ichimura, K. Cell division and expansion in petals during flower development and opening in *Eustoma grandiflorum*. *Hort. J.* **85**, 154–160. https://doi.org/10.2503/hortj.MI-071 (2016).
25. Du, H. et al. Characterisation of flower colouration in 30 *Rhododendron* species *via* anthocyanin and flavonol identification and quantitative traits. *Plant Biol.* **20**, 121–129. https://doi.org/10.1111/plb.12649 (2017).
26. Nabipour Sanjbod, R., Chamani, E., Pourbeyrami Hir, Y. & Estaji, A. Autophagic and phytochemical aspects of color changes in white petals of snapdragon flower during development and senescence. *Physiol. Mol. Biol. Plants.* **29**, 695–707. https://doi.org/10.1007/s12298-023-01323-7 (2023).
27. Hong, S. D. et al. Decoding the formation of diverse petal colors of *Lagerstroemia indica* by integrating the data from transcriptome and metabolome. *Front. Plant Sci.* **13**, 970023. https://doi.org/10.3389/fpls.2022.970023 (2022).
28. Aghhavani Shajari, M. & Rezvani Moghaddam, P. Are the apocarotenoids content and colorimetric traits of saffron (Crocus sativus L.) affected by some post harvesting operations?. *J. Stored Prod. Res.* **97**, 101967. https://doi.org/10.1016/j.jspr.2022.101967 (2022).
29. Nabipour Sanjbod, R., Chamani, E., Pourbeyrami Hir, Y. & Estaji, A. Autophagic and phytochemical aspects of color changes in white petals of snapdragon flower during development and senescence. *Physiol. Mol. Biol. Pla.* **29**, 695–707. https://doi.org/10.1007/s12298-023-01323-7 (2023).
30. Wang, R. et al. Integrated metabolomics and transcriptome analysis of flavonoid biosynthesis in safflower (Carthamus tinctorius L.) with different colors. *Front. Plant Sci.* **12**, 712038. https://doi.org/10.3389/fpls.2021.712038 (2021).
31. Peng, J. Q., Dong, X. J., Xue, C., Liu, Z. M. & Cao, F. X. Exploring the molecular mechanism of blue flower color formation in hydrangea macrophylla cv. "forever summer". *Front. Plant Sci.* **12**, 585665. https://doi.org/10.3389/fpls.2021.585665 (2021).
32. Hua, M. et al. Determination of anthocyanins and flavonols in paeonia delavayi by high-performance liquid chromatography with diode array and mass spectrometric detection. *Anal. Lett.* **15**, 2331–2339. https://doi.org/10.1080/00032719.2017.1423322 (2018).
33. Wu, Q. et al. Relationship between the flavonoid composition and flower colour variation in Victoria. *Plant Biol.* **20**, 674–681. https://doi.org/10.1111/plb.12835 (2018).
34. Ohmiya, A., Hirashima, M., Yagi, M., Tanase, K. & Yamamizo, C. Identification of genes associated with chlorophyll accumulation in flower petals. *PLoS one.* **9**, e113738. https://doi.org/10.1371/journal.pone.0113738 (2014).
35. An, X. et al. Physiological response of anthocyanin synthesis to different light intensities in blueberry. *PloS one.* **18**, e0283284. https://doi.org/10.1371/journal.pone.0283284 (2023).
36. Zhou, Q., Zhao, F., Zhang, H. H., Zhu, Z. L. & Tang, P. Variation of flower color during the flowering period of *Nymphaea hybrid*. *Chinese J. Trop. Crops.* **45**, 122–133 (2024).
37. Wang, H. C., Huang, X. M., Hu, G. B. & Huang, H. B. Studies on the relationship between anthocyanin biosynthesis and related enzymes in *Litchi* pericarp. *Scientia Agricult. Sinica.* **12**, 2028–2032 (2004).

38. Meng, L. S. et al. Sucrose signaling regulates anthocyanin biosynthesis through a MAPK Cascade in *Arabidopsis thaliana*. *Genetics.* **210**, 607–619. https://doi.org/10.1534/genetics.118.301470 (2018).
39. Fernandes, L., Pereira, J. A., Saraiva, J. A., Ramalhosa, E. & Casal, S. Phytochemical characterization of Borago officinalis L. and Centaurea cyanus L. during flower development. *Food Res. Int.* **123**, 771–778. https://doi.org/10.1016/j.foodres.2019.05.014 (2019).
40. He, Y. Q., Ma, L. Y. & Sang, Z. Y. Preliminary study on formation of flower color in *Magnolia wuf engensis*. *Acta Botanica Boreali-Occidentalia Sinica.* **30**, 2252–2257 (2010).
41. Gao, S., Liu, J., Tang, Y. Q., Tang, Z. H. & Zhang, J. Analysis on the key physicochemical properties of the coloration of varietals of *Catharanthus roseus*. *Non-wood Forest Res.* **40**, 214–227 (2022).
42. Saidji, N., Malki, F., Boukerche, H. & Mokrane, H. Insight into stability and degradation kinetics of Roselle (*Hibiscus sabdariffa* L.) flowers anthocyanin, effect of pH, heating, storage conditions, and co-pigment treatment. *Biomass Conv. Bioref.* **14**, 30613–30625. https://doi.org/10.1007/s13399-023-04946-8 (2024).
43. Wang, Y. S. et al. New insight into the pigment composition and molecular mechanism of flower coloration in tulip (Tulipa gesneriana L.) cultivars with various petal colors. *Plant Sci.* **317**, 111193. https://doi.org/10.1016/j.plantsci.2022 (2022).
44. Whitney, H. M. et al. Why do so many petals have conical epidermal cells?. *Ann. Bot.* **108**, 609–616. https://doi.org/10.1093/aob/mcr065 (2011).
45. Stavenga, D. G., Staal, M. & van der Kooi, C. J. Conical epidermal cells cause velvety colouration and enhanced patterning in Mandevilla flowers. *Faraday Discuss.* **223**, 98–106. https://doi.org/10.1039/d0fd00055h (2020).
46. Liu, A. C. et al. Changes of floral color and pigment content during flowering in several species of *Lonicera* L. *J. Southwest (Natural Science Edition).* **42**, 22–29 (2020).
47. Brouillard, R. The in vivo expression of anthocyanin colour in plants. *Phytochemistry* **22**, 1311–1323. https://doi.org/10.1016/s0031-9422(00)84008-x (1983).

Author contributions

All authors have read and agreed to the published version of the manuscript. S.D., W.F. and J.C. conceived and designed the work. W.F., Y.Z., J.Y. and J.F. collected the data. W.F. analyzed and interpreted the data. W.F. drafted the manuscript. S.D., J.C. and Y.S. revised the manuscript.

Funding

This research was funded by the Liaoning Province Wild apricot Germplasm Resource Preservation and Breeding National Permanent Scientific Research Base [Grant No. 2020132519], and the Innovation Team for Creating and Utilizing Non-wood Forest Germplasm Resources in Semi-arid Regions of National Forestry and Grassland Administration.

Declarations

Competing interests

The authors declare no conflict of interest.

Additional information

Supplementary Information The online version contains supplementary material available at https://doi.org/10.1038/s41598-025-91280-w.

Correspondence and requests for materials should be addressed to J.C. or S.D.